

Direct mineralogical composition of a MgO-C refractory material obtained by Rietveld methodology

Ángeles G. De la Torre^a, Francisco José Valle^b, Antonio H. De Aza^{b,*}

^a *Departamento de Química Inorgánica, Cristalografía y Mineralogía, Universidad de Málaga, 29071 Málaga, Spain*

^b *Instituto de Cerámica y Vidrio, Consejo Superior de Investigaciones Científicas (CSIC), Campus de Cantoblanco, c/ Kelsen 5, 28049 Madrid, Spain*

Received 27 January 2005; received in revised form 19 May 2005; accepted 24 May 2005

Available online 2 August 2005

Abstract

Magnesia-graphite refractory materials are used in large quantities in the steelmaking process. The chemical characterization of this type of refractories is an arduous task that requires a rigorous set of laboratory tests and analyses. In the present paper, proper characterization of magnesia-graphite refractories has been approached by X-ray powder diffraction combined with Rietveld methodology. The quantitative phase analysis of a MgO-graphite refractory has been 68.3 wt% of MgO, 8.1 wt% of graphite, 13.5 wt% of Al₂O₃, 4.4 wt% of SiC, 0.6 wt% of Si, 1.2 wt% of Al, 1.5 wt% of AlPO₄ and 2.4 wt% of silicone. These results have been checked and validated with those obtained by other analysis procedures used to determine the crystalline and non-crystalline phases present in these materials.

© 2005 Elsevier Ltd. All rights reserved.

Keywords: Refractories; MgO-C refractories; X-ray methods; Rietveld; Analysis

1. Introduction

Magnesia-graphite materials are an established refractory for the steel industry.¹ The excellent properties of various forms of carbon in refractories have been well known among industry experts for a long time. In the 1980s significant amounts of these materials were used in Japan,^{2–7} but it was later on in the United States where products were developed and launched in response to demand arising from new processes in the metallurgical industry and advances in refractory technology.⁸

Magnesia-graphite refractories are characterised by excellent corrosion resistance due to their low wettability by fluid slag and metal; high resistance to thermal shock as a result of the graphite content that increases the thermal conductivity and reduces the thermal expansion; and good mechanical strength at high temperatures. The ease of oxidation by air, water or carbon dioxide at high temperatures is one of the

main drawbacks of these materials. Therefore, they are commonly used in reducing atmospheres.

Originally, these materials were constituted by periclase (MgO), graphite (C) and aluminium (Al),^{9,10} but in recent years, magnesia-carbon materials have been the subject of several projects aimed at improving their mechanical, thermal and chemical properties and reducing hazardous emissions during fabrication as well as during steel processing. Nowadays the anti-oxidation role of the aluminium is being enhanced by the addition of silicon (Si) or even, silicon carbide (SiC).^{11,12} The composition of high-duty magnesia-carbon bricks has been improved in recent years, essentially in terms of the binders used.¹ Currently, the addition of some polysiloxane (silicone) as a binder is usual.¹³

Proper mineralogical characterization of a magnesia-graphite material is vital for its quality control and to understand its final performance. This is an arduous problem that requires a rigorous set of laboratory tests and analyses since C, Si and Al elements coexist with SiC (non-oxide inorganic phase) jointly with organic phases (polysiloxanes), oxide phases (MgO, Al₂O₃), berlinite (AlPO₄), some additives and

* Corresponding author.

E-mail address: aaza@icv.csic.es (A.H. De Aza).

impurities. So, magnesia-graphite refractories must be considered as very complex materials.

In the scientific bibliography there is lack of information about a methodology to obtain a magnesia-graphite full-material chemical analysis. However, there are numerous papers that report the single analysis of each one of the components.^{14–27} In a previous work the authors have developed a methodology that makes possible a whole analysis of these type of materials.²⁸

The goal of the present investigation is to approach the aforementioned problem by X-ray powder diffraction (XRPD) combined with Rietveld methodology.²⁹ This method is one of the most useful tools to obtain Quantitative Phase Analyses, QPA, directly. The method is standardless but the crystal structures of all the phases present in the sample must be known as the process comprises the comparison of the measured and calculated patterns. Rietveld QPA has been successfully applied to simple mixtures^{30,31} and in the last years it has been employed to more complex industrial materials such as ordinary Portland clinkers and cements,^{32–34} calcium aluminate cements,³⁵ mineralised Portland clinkers³⁶ and porcelains.³⁷ This methodology has several advantages over others because it uses a wide diffraction range minimizing peak overlap, preferred orientation and sample broadening effects.^{38,39} The quantification of amorphous content within a given material is also possible using Rietveld methodology by adding a suitable internal standard.⁴⁰ The results obtained by this methodology for a MgO-graphite refractory have been validated with those obtained by other analysis procedures that make it possible to determine the crystalline and non-crystalline phases present in these materials.

2. Experimental procedure

2.1. X-ray data collection

A magnesia-graphite sample ground to less than 35 μm was characterised by XRPD at room temperature. The powder pattern was collected on a Siemens D5000 automated diffractometer using graphite-monochromated Cu $K\alpha_{1,2}$ radiation (1.5418 Å). The diffractometer optic used to collect the sample was: a fixed aperture slit of 2 mm, one scattered-radiation

slit of 2 mm after the pattern, followed by a system of secondary Soller slits and the detector slit of 0.2 mm. The pattern was recorded between 5° and 80° (2 θ) in 0.03° steps, counting 20 s per step. The sample was rotated at 15 rpm during data collection.

2.2. Rietveld refinement

Rietveld refinement was done using the GSAS suite of programs.⁴¹ Peak shape for every phase was modelled by a pseudo-Voigt function⁴² including the asymmetry correction of Finger et al.⁴³ March-Dollase algorithm⁴⁴ was used to correct the preferred orientation effect when it was observed, e.g. graphite along [001] direction.

The bibliographic references for the crystal structures descriptions used to calculate powder patterns are given in Table 1.^{45–52} The linear absorption coefficients for Cu $K\alpha_{1,2}$ radiation are also listed. When anisotropic vibration temperature factors were reported, these were converted to the corresponding isotropic values and introduced in the Rietveld analysis. Optimised parameters in final refinement were: background coefficients, cell parameters, zero shift error, peak shape parameters, preferred orientation (when appropriate), and phase fractions.

2.3. Chemical analysis methodologies

XRPD, differential thermal analysis (DTA) and thermogravimetry analysis (TG), infrared spectrometry (FT-IR), chemical analysis by inductive coupled plasma-atomic emission spectroscopy (ICP-AES), flame photometry (FP) and induction furnace carbon/sulphur analyzer (LECO) are a set of techniques suitable to approach these types of analyses.

The following equipments and operating conditions were used: *DTA and TG*: a STA-490 Netzsch was used to heat the specimens in platinum crucibles to 1400 °C at a heating rate of 10 °C min⁻¹, in a flow of dry air. *FT-IR* spectra were recorded over the 400–4000 cm⁻¹ spectral range with Fourier transformed data using a Perkin-Elmer 1760X spectrophotometer. The operating conditions were: 4 cm⁻¹ resolution, 10 scans, 0.4 mV laser energy, 2000:1 resolution power. *ICP-AES*: a Thermo Jarrell Ash IRIS Advantage axial plasma spectrometer with computer controlled polychromator to analyse a pre-defined wavelength range was used. The source was pow-

Table 1
Some structural details of the investigated phases

Mineral name	Chemical formula	μ^a	PDF file number	ICSD collection code	Bibliographic reference
Periclase	MgO	99.4	43–1022	9863	45
Graphite	C	9.3	41–1487	76767	46
Corundum	Al ₂ O ₃	121.1	43–1484	73725	47
Silicon carbide	SiC	139.8	29–1131	15325	48
Silicon	Si	139.3	27–1402	60389	49
Aluminium	Al	129.6	04–0787	44321	50
Berlinite	AlPO ₄	91.1	10–0423	66999	51,52

^a Linear absorption coefficient, μ , in cm⁻¹.

ered by 2 kW crystal controlled radiofrequency generator operating at 40.68 MHz. An especial detection configuration with 262,144 individually addressable detector elements in a 512×512 array allows the continuous coverage of the available wavelength ranges. *FP*: A 2100 Perkin-Elmer atomic absorption spectrometer was used in flame emission spectrophotometer mode to perform the flame emission spectrometry. *LECO CS-200*: The equipment has an induction furnace that allows sample combustion.

2.4. Microstructural examination

To study the microstructure of the material several cross-sections of the refractories were mounted in epoxy resins and were progressively diamond polished down to 1 μm . Phase identification was performed using reflected-light microscopy (RLM) (Carl Zeiss Axiophot Stereomicroscope) and phase analysis was carried out using a field emission scanning electron microscope (FESEM) (Hitachi-S4700) fitted with an energy-dispersive spectrometer (Noran System Six-Thermo Electron Corporation).

3. Results and discussion

3.1. Rietveld quantitative phase analysis

A mineralogical phase identification was initially carried out. The sample contains seven crystalline phases: periclase (MgO), graphite (C), corundum (Al_2O_3), silicon carbide (SiC), silicon (Si), aluminium (Al) and berlinite (AlPO_4). Graphite showed preferred orientation that must be corrected. March Dollase algorithm along $[001]$ was used and the refined parameter converged to 0.58(2) (a value of 1.0 represents an ideal “random” powder). To obtain accuracy, QPA microabsorption effect should be borne in mind. This effect may be important if the linear absorption coefficient of any phase, in a mixture, is different from that of the mixture and the particle size distribution is not homogeneous. The average linear absorption coefficient of this material is 104 cm^{-1} approximately, and the C coefficient is the farthest value from it, see Table 1. A method to partially correct this effect was developed by Brindley⁵³ and related to the Rietveld methodology by Taylor.⁵⁴ A detailed description of this correction has recently been presented.⁵⁵ As will be seen, Rietveld QPA results and the results of other methods match satisfactorily (Table 3). Hence, the microabsorption effect does not seem to be a problem in the present case and its correction is likely not needed. Final R_{WP} disagreement factor⁵⁶ converged to 10.3% indicating a good fit; see also the flatness of the difference curve in Fig. 1. In this figure, the Rietveld plot for the refractory is shown ($20\text{--}80^\circ/2\theta$) with main peaks for each phase labelled. Furthermore, the values of the phase-dependent, R_{F} , disagreement factor⁵⁶ are small, see Table 2, which indicates that fits to any given phase are satisfactory. Rietveld QPA results are given in Table 2.

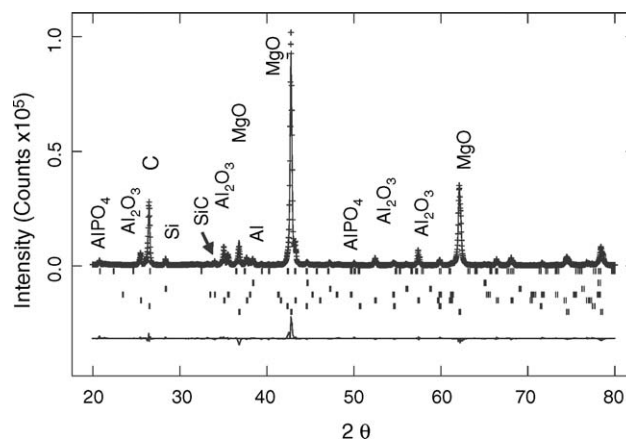


Fig. 1. Rietveld plot ($20\text{--}80^\circ/2\theta$) for the analysed Mg-C refractory with main peaks of each phase labelled. Observed (crosses), calculated (line) and difference (bottom line) powder patterns are shown. The marks correspond to the Bragg peaks of the different phases, from bottom to top: MgO, C (graphite), Al_2O_3 , SiC, Si, Al and AlPO_4 .

Table 2
Rietveld refinement results for the MgO-C refractory material

Phase	Wt% ^a	R_{F} (%)
MgO	70.1 (1)	3.8
C (graphite)	8.3 (6)	5.1
Al_2O_3	13.8 (1)	3.2
SiC	4.5 (1)	7.2
Si	0.6 (3)	5.8
Al	1.2 (1)	5.3
AlPO_4	1.5 (1)	12.0

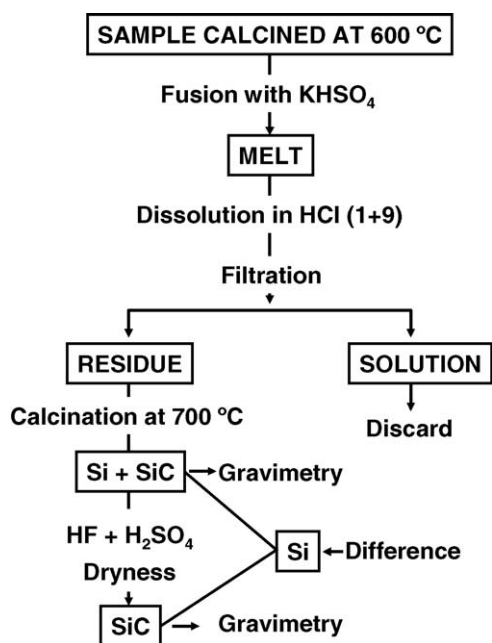
^a Figures between parentheses: standard deviation (σ) derived from the phase fraction given by the Rietveld least-squares analysis.

Rietveld results, shown in Table 2, are normalized to 100% of crystalline fraction, so the hypothetical amorphous and organic content of the sample is assumed to be negligible. Bearing in mind that the material contains 2.4 wt% of silicone acting as a binder, determined by TG and LECO,²⁸ data obtained by Rietveld must be fitted to 97.6 wt%, as is shown in Table 3. These results have been compared with those

Table 3
Rietveld quantitative phase analysis for a magnesia-graphite refractory material vs. other methods results

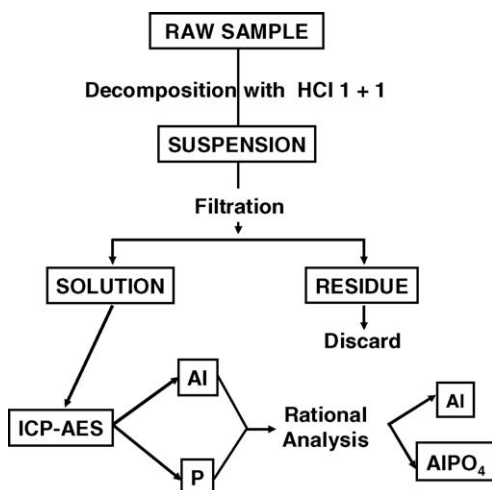
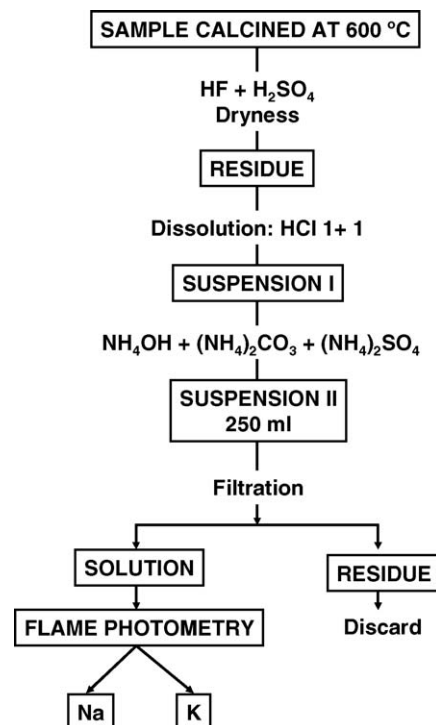
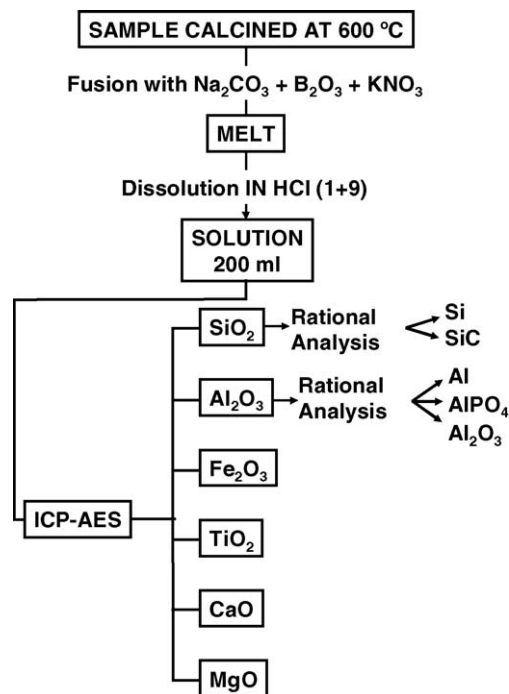
Phase	Rietveld QPA Wt% (up to 97.6%)	Other methods results	
		Wt% ^a	Method
MgO	68.3	64.1 (3)	ICP-AES
C (graphite)	8.1	9.0 (3)	LECO
Al_2O_3	13.5	12.7 (2)	ICP-AES
SiC	4.4	4.4 (2)	Gravimetry and LECO
Si	0.6	1.5 (1)	Gravimetry
Al	1.2	2.21 (5)	ICP-AES
AlPO_4	1.5	0.8 (1)	ICP-AES
Silicone (polyxiloxane)	–	2.4	TG

^a Figures between parentheses: standard deviation (σ) derived from five replicates (precision of the method).

Fig. 2. Procedure scheme for determination of silicon and silicon carbide.²⁸

obtained, following the described procedures (Figs. 2–5), by other methods.²⁸ As can be seen, Rietveld QPA and results from other methods match satisfactorily (see Table 3) and therefore it can be assumed that the amorphous phase content in the material (that includes every minor crystalline phase not defined, all non-diffracting fractions such as vitreous phases, grain boundary regions, intrinsic defects, etc.) is negligible. To confirm this point, the microstructure of the refractory was studied. Fig. 6 shows a reflected light optic microscope image of the MgO-C material, where no significant amount of glassy phase can be detected.

To put it more precisely, the difference observed for the MgO weight content (68.3/64.1) has sense due to the high amount of this phase in the refractory. In comparison, the results shown in Table 3 for Al (1.2/2.21) have a rela-

Fig. 3. Procedure scheme for determination of Al and AlPO₄.²⁸Fig. 4. Procedure scheme for determination of alkalis.²⁸Fig. 5. Procedure scheme for determination of all the remaining components.²⁸

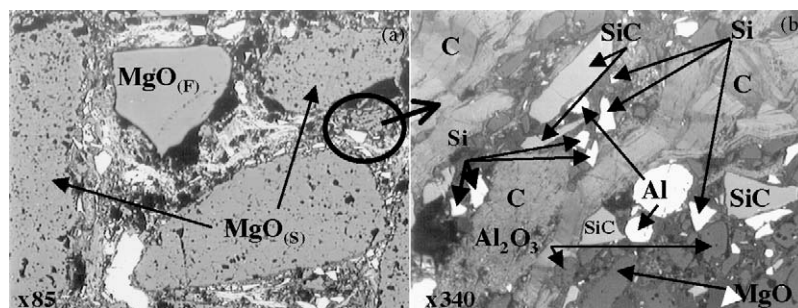


Fig. 6. Reflected light optic microscope images of the microstructure of the MgO-C refractory: (a) low magnification image ($\times 85$) and (b) higher magnification image ($\times 380$) showing a selective magnification of the refractory matrix. The main phase identified are labelled: $\text{MgO}_{(F)}$: fused magnesite, $\text{MgO}_{(S)}$: sintered magnesite, C: graphite, Al_2O_3 : corundum, SiC: silicon carbide, Si: silicon and Al: aluminium. No significant amount of glassy phase can be detected.

tively large inaccuracy. In this particular case, the 2.21-value reported for Al was deduced by rational analysis from P and Al data obtained by ICP-AES (Fig. 3). So the aforementioned data is affected by a larger error than 1.2-Rietveld data for Al. It is worth to mention that the chemical analysis gives the existence of some impurities (wt%): $\text{Fe}_2\text{O}_3 = 0.20(2)$ (ICP-AES); $\text{TiO}_2 = 0.02(2)$ (ICP-AES); $\text{CaO} = 1.40(4)$ (ICP-AES); $\text{Na}_2\text{O} = 0.070(5)$ (FE); $\text{K}_2\text{O} = 0.19(2)$ (FE); silica = 2.4 (TG); moisture = 0.5 (TG).

4. Conclusions

The following concluding remarks can be made:

- The analysed MgO-graphite refractory material is composed by: MgO (68.3 wt%), C (graphite: 8.1 wt%), Al_2O_3 (13.5 wt%), SiC (4.4 wt%), Si (0.6 wt%), Al (1.2 wt%), AlPO_4 (1.5 wt%) and silicone (2.4 wt%).
- Rietveld quantitative phase analysis using laboratory X-ray powder diffraction is a suitable methodology to directly obtain the mineralogical composition of MgO-graphite refractories.
- This methodology is appropriated to be applied to quality control and to understand final performances of this type of materials.

Acknowledgments

The authors acknowledge the contribution of Miguel A.G. Aranda, and Salvador De Aza in offering valuable suggestions and stimulating discussion during the course of this work.

References

- Aneziris, C. G., Borzov, D. and Ulbricht, J., Magnesite-carbon bricks: a high-duty refractory material. *Interceram. Refract. Manual.*, 2003, 22–27.
- Hayashi, T., Recent development of refractories technology in Japan. In *Proceeding of The First International Conference on Refractories*.

- Technical Association of Refractories of Japan, Tokyo, Japan, 1983, pp. 5–33.
- Ishibashi, T., Matsumura, T., Hosokawa, K. and Matsomota, K., Behaviours of flake graphites on magnesite clinkers in magnesite-carbon refractories. *Taikabutsu Overseas*, 1983, 3(4), 3–13.
- Nameishi, N., Influence of magnesite clinker on the properties of unburned magnesite-carbon bricks [translation]. *Taikabutsu* 1980, 32, 583–587.
- Watanabe, A. and Takeuchi, Y., Application of magnesite-carbon bricks to converter lining. *Taikabutsu Overseas*, 1981, 1(1), 40–48.
- Kyoden, H., Nishio, H. and Matsumoto, T., Magnesite-carbon tuyere bricks for combined blowing in LD converter. *Taikabutsu Overseas*, 1983, 3(1), 10–16.
- Naruse, Y., Fujimoto, S., Kamada, Y. and Abe, M., Results of investigation of magnesite-carbon bricks used in converter. *Taikabutsu Overseas*, 1983, 3(2), 3–7.
- Moore, R.E., Advance in American refractory science and technology in response to steelmaking practice over the period of 1925-present. In *Proceeding of the 7th Steelmaking Conference*. The Iron and Steel Society of the AIME, Toronto, Canada, 1992, pp. 139–145.
- Watanabe, A., Matsuki, T., Takahashi, H. and Takahashi, M., Effect of metallic element addition on the properties of magnesite-carbon bricks. In *Proceeding of The First International Conference on Refractories: Refractories for the Steel Industry*. Technical Association of Refractories of Japan, Tokyo, Japan, 1983, pp. 125–134.
- Brant, P.O.C.R. and Rand, B., Reaction of silicon and aluminium in MgO-graphite composites: I. Effect on porosity and microstructure. In *Proceeding of The UNITECR'91 Congress* (2nd ed.). The German Refractories Association, Bonn, Germany, 1991, pp. 247–250.
- Murata, K., Matsui, T. and Kono, K., Oxidizing prevention of MgO-C bricks for converter. *Taikabutsu Overseas*, 1991, 11(2), 17–22.
- Yamaguchi, A. and Tanaka, H., Role and behaviour of non-oxide compounds added to carbon-containing refractories. In *Proceeding of The UNITECR'91 Congress* (2nd ed.). The German Refractories Association, Bonn, Germany, 1991, pp. 32–38.
- ALFRAN S.A., personal communication, 2004.
- Bennet, H. and Reed, R.A., *Chemical Methods of Silicate Analysis*. Academic Press, Inc. London Ltd., 1971, pp. 102–112.
- International Organization for Standardization. ISO 100058 (1992). U.E. version (1996).
- American Society for Testing and Materials. Withdrawn Standard: C574-84. Withdrawn (1993).
- Criado, E., Barba, M^a. F. and Cardin, J. M., Caracterización de grafitos empleados en refractarios. *Bol. Soc. Esp. Ceram.* V., 1989, 28(2), 105–115.
- American Society for Testing and Materials. Withdrawn Standard: C571-81. Withdrawn (1995).
- Deutsches Institut für Normung. DIN 51075 (1982).

20. Prost, L. and Pauillac, A., Contribution à la détermination de la teneur en SiC pur du carbure de silicium et des produits à base de carbure de silicium. *Bull. Soc. Fr. Ceram.*, 1969, **84**, 75–83.
21. Franek, M. and Krivan, V., Multielement characterization of silicon carbide powders by instrumental neutron activation analysis and ICP-atomic emission. *Fresenius J. Anal. Chem.*, 1992, **342**, 118–124.
22. Shen, R. and Chen Aix, M., In *Proceeding 6th International Symposium on Science and Technology*, 1995, pp. 130–135.
23. Julietti, R., A scheme of analysis for silicon carbide refractories. *Trans. J. Br. Ceram. Soc.*, 1981, **80**, 175.
24. Florian, K., Fisher, W. and Nickel, H., Direct solid sample analysis of silicon carbide powders by direct current glow discharge and direct current arc emission spectrometry. *J. Anal. At. Spectrom.*, 1994, **9**, 257–262.
25. Docekul, B., Broekaert, J. A. C., Graule, F., Tschöpel, P. and Tolg, G., Determination of impurities in silicon carbide powders. *Fresenius J. Anal. Chem.*, 1992, **342**, 113.
26. Baudin, C., Alvarez, C. and Moore, R., Influence of chemical reactions in magnesia-graphite refractories: I. Effects on texture and high-temperature mechanical properties. *J. Am. Ceram. Soc.*, 1999, **82**(12), 3529–3567.
27. Baudin, C., Alvarez, C. and Moore, R., Influence of chemical reactions in magnesia-graphite refractories: II. Effects of aluminum and graphite contents in generic products. *J. Am. Ceram. Soc.*, 1999, **82**(12), 3539–3587.
28. De Aza, A.H., Valle, F.J., Ortega, P., Pena, P. and De Aza, S., Analytical characterization of a magnesia-graphite refractory. Internal reporting, 2005.
29. Rietveld, H. M., A profile refinement method for nuclear and magnetic structures. *J. Appl. Crystallogr.*, 1969, **2**, 65–71.
30. Hill, R. J. and Howard, C. J., Quantitative phase analysis from neutron powder diffraction data using the Rietveld method. *J. Appl. Crystallogr.*, 1987, **20**, 467–474.
31. Bish, D. L. and Howard, S. A., Quantitative phase analysis using the Rietveld method. *J. Appl. Crystallogr.*, 1988, **21**, 86–91.
32. Taylor, J. C., Hinczak, I. and Matulis, C. E., Rietveld full-profile quantification of Portland clinker: the importance of including a full crystallography of the major phase polymorphs. *Powder Diffr.*, 2000, **15**, 7–18.
33. De la Torre, A. G., Cabeza, A., Calvente, A., Bruque, S. and Aranda, M. A. G., Full phase analysis of Portland clinker by penetrating synchrotron powder diffraction. *Anal. Chem.*, 2001, **73**, 151–156.
34. De la Torre, A. G., Bruque, S., Campo, J. and Aranda, M. A. G., The superstructure of C₃S from synchrotron and neutron powder diffraction and its role in quantitative phase analyses. *Cem. Concr. Res.*, 2002, **32**, 1347–1356.
35. Guirado, F., Galf, S. and Chinchón, S., Quantitative Rietveld analysis of aluminous cement clinker phases. *Cem. Concr. Res.*, 2000, **30**, 1023–1029.
36. Pajares, I., De la Torre, A. G., Martínez-Ramírez, S., Puertas, F., Blanco-Varela, M. T. and Aranda, M. A. G., Quantitative analysis of mineralized white Portland clinkers: the structure of Fluorellestadite. *Powder Diffr.*, 2002, **17**(4), 281–286.
37. De Aza, A. H., De la Torre, A. G., Aranda, M. A. G. and De Aza, S., Quantitative Rietveld analysis of Buen Retiro Porcelains. *J. Am. Ceram. Soc.*, 2004, **87**(3), 449–454.
38. Madsen, I. C., Scarlett, N. V. Y., Cranswick, L. M. D. and Lwin, T., Outcomes of the International Union of Crystallography Commission on powder diffraction round robin on quantitative phase analysis: samples 1a to 1h. *J. Appl. Crystallogr.*, 2001, **34**, 409–426.
39. Scarlett, N. V. Y., Madsen, I. C., Cranswick, L. M. D., Lwin, T., Groleau, E., Stephenson, G., Aylmore, M. and Agron-Olshina, N., Outcomes of the International Union of Crystallography Commission on powder diffraction round robin on quantitative phase analysis: samples 2, 3, 4, synthetic bauxite, natural granodiorite and pharmaceuticals. *J. Appl. Crystallogr.*, 2002, **35**, 383–400.
40. De la Torre, A. G., Bruque, S. and Aranda, M. A. G., Rietveld quantitative amorphous content analysis. *J. Appl. Crystallogr.*, 2001, **34**, 196–202.
41. Larson, A.C. and Von Dreele, R.B., *GSAS Program*. Los Alamos National Lab. Rep. No. LA-UR-86748, 1994.
42. Thompson, P., Cox, D. E. and Hasting, J. B., Rietveld refinement of Debye–Scherrer synchrotron X-ray data from Al₂O₃. *J. Appl. Crystallogr.*, 1987, **20**, 79–83.
43. Finger, L. W., Cox, D. E. and Jephcoat, A. P., A correction for powder diffraction peak asymmetry due to diaxial divergence. *J. Appl. Crystallogr.*, 1994, **27**, 892–900.
44. Dollase, W. A., Correction of intensities for preferred orientation in powder diffractometry: application of the March model. *J. Appl. Crystallogr.*, 1986, **19**, 267–272.
45. Sasaki, S., Fujino, K. and Takeuchi, Y., X-ray determination of electron-density distributions in oxides, MgO, MnO, CoO, and NiO, and atomic scattering factors of their constituent atoms. In *Proceedings of Japan Academy* 55, 1979, pp. 43–48.
46. Trucano, P. and Chen, R., Structure of graphite by neutron-diffraction. *Nature*, 1975, **258**, 136–137.
47. Maslen, E. N., Streltsov, V. A., Streltsova, N. R., Ishizawa, N. and Satow, Y., Synchrotron X-ray study of the electron-density in α -Al₂O₃. *Acta Crystallogr.*, 1993, **B49**, 973–980.
48. Gomes de Mesquita, A. H., Refinement of the crystal structure of SiC type 6H. *Acta Crystallogr.*, 1967, **23**, 610–617.
49. Batchelder, D. N. and Simmons, R. O., Lattice constants and thermal expansivities of silicon and of calcium fluoride between 6 degrees and 322 degrees K. *J. Chem. Phys.*, 1964, **41**, 2324–2329.
50. Straumanis, M. E., Absorption correction in precision determination of lattice parameters. *J. Appl. Phys.*, 1959, **30**, 1965–1969.
51. Muraoka, Y. and Kihara, K., The temperature dependence of the crystal structure of berlinite, a quartz-type form of AlPO₄. *Phys. Chem. Miner.*, 1997, **24**, 243–253.
52. Natl. Bur. Stand. (U.S.). Circ. 539. 10. 3 (1960).
53. Brindley, G. W., The effect of Grain or particle size on X-ray reflection from mixed powders and alloys, considered in relation to the quantitative determination of crystalline substances by X-ray methods. *Philos. Mag.*, 1945, **36**, 347–369.
54. Taylor, J. C., Computer programs for standardless quantitative analysis of minerals using the full powder diffraction profile. *Powder Diffr.*, 1991, **6**(1), 2–9.
55. Winburn, R. S., Lerach, S. L., Jarabek, B. R., Wisdom, M. A., Grier, D. G. and McCarthy, G. J., Quantitative XRD analysis of coal combustion by-products by the Rietveld method. Testing with standard mixtures. *Adv. X-ray Anal.*, 1998, **42**, 387–396.
56. Young, R. A., *The Rietveld Method*. Oxford University Press, 1993.